# Eye-tracking in aviation: a new method for detecting learned visual scan patterns of cockpit instrument in simulated flight

**Conference Paper**

**Author(s):**
Brams, Stephanie; Rejtman, Rafaël F.; Levin, Oron; Ziv, Gal; Hooge, Ignace TC; Helsen, Werner F.

**Publication date:**
2020-03

**Permanent link:**
https://doi.org/10.3929/ethz-b-000407654

# Eye-tracking in aviation: a new method for detecting learned visual scan patterns of cockpit instrument in simulated flight

Stephanie Brams[✉1], Rafaël F. Rejtman[2], Oron Levin[1], Gal Ziv[3], Ignace TC Hooge[4], and Werner F. Helsen[1]

[1]Movement Control & Neuroplasticity Research Group, KU Leuven, Leuven, Belgium
[2]Engineering School, University of São Paolo, Brazil
[3]The Academic College at Wingate, Wingate Institute, Netanya, Israel
[4]Utrecht University, Experimental Psychology, Utrecht, The Netherlands

Piloting an aircraft requires that various tasks be completed concurrently in an efficient manner. Here we present an algorithm that was developed with the intent of examining whether instructed scan patterns (i.e., the order of fixations on cockpit instruments in specific flight maneuvers) were followed by student pilots during a simulated flight. Participants were scored based on matching between actual scan patterns and instructed scan patterns. Both foveal and parafoveal scanning patterns were analyzed. For foveal scanning, patterns were detected based on fixations on instrument locations. For parafoveal scanning, patterns were detected based on gradient masks over the instruments, indicating a probability score about the instrument that was possibly fixated. For future perspectives, the algorithm could serve for development of a real-time feedback cockpit layout to alarm when scan patterns are suboptimal. Integrating a scan-pattern monitoring device in the cockpit is expected to reduce pilot-related accidents and incidents.

*Keywords & Phrases:* Scan patterns, Instrumented flight, Basic flying assessment test, Training

## 1 INTRODUCTION

The effects of gaze behavior on flight performance in pilots has been examined in previous studies [1, 2]; for a recent review, see [3]. Optimal visual attention to cockpit instruments allows pilots to extract the relevant information needed to support skilled decision making while flying the aircraft or monitoring its automated flight computers [4–6]. In commercial aircraft equipped with modern automated technologies, pilots spend more time monitoring instruments rather than physically flying the aircraft [7, 8]. Hence, being able to detect changes in the state of the aircraft, and specifically, being able to detect malfunctions is of importance. Ineffective monitoring of aircraft instruments was a contributing factor in many flight accidents [9]. A tragic example was the 2009 crash of Colgan Air flight 3407. Here, a major contributing factor to this fatal accident was "the flight crew's failure to monitor airspeed in relation to the rising position of the low-speed cue" [10]. The development of modern eye-tracking technologies presents an opportunity to "monitor the monitoring" ([8] abstract). Eye-tracking information can, for example: (1) give flight instructors more information to improve teaching in a simulator, (2) supplement the data already recorded in the flight recording system ("black box") and provide useful information for accident analysis, and (3) follows pilots' gaze in real time and provide useful alerts when visual attention is not optimal [8]. While some of these implementations of eye-tracking technologies is still in early stages of design, there is a need to create algorithms and analysis tools that will allow researchers and practitioners to gain insights from the recorded eye-tracking data. Implementing eye-tracking in pilot training and using it for flight performance analysis can allow flight

✉Contact: stephanie.brams@kuleuven.be

instructors to optimize the monitoring capabilities of student pilots [8]. Development of analysis tools that could provide information about the relationship between pilots' visual scanning and his/her situation awareness, decision making, and flight performance at the early stage of flight training is therefore desirable.

In this methodological paper we will describe two innovative visual scoring models to quantify scan patterns used in the cockpit. The first model (**Model 1**) is designed to examine matching between actual and instructed visual scanning of cockpit instrument during performance of various flight maneuvers. Since pilots are expected to use both their foveal and parafoveal vision during scanning of the cockpit instruments they may not always fixate directly on an instrument but rather fixate on the spaces between instruments. Therefore, in the second model (**Model 2**) we use an algorithm that predicts the probability of an instrument to be scanned for a given point of gaze. The integration of both into a unified assessment algorithm is expected to provide insights on visual scanning behavior of pilots from raw eye-tracking data that may be otherwise meaningless. The two models were implemented in a case study where visual scanning patterns of student pilot were analyzed before and after training sessions of a simulated flight.

## 2 MATERIALS AND METHODS

Gaze data were generated by the Tobii Pro Glasses 2 eye-tracker (Tobii Technology AB, Sweden). The gaze points exported from the glasses, nevertheless, contained coordinates associated with the moving (non-inertial) reference frame of the glasses themselves and needed to be transferred to a fixed coordinate system. Fixations were mapped on a static image of the Garmin G1000 instrument panel, using the "Real-World Mapping" tool provided by the Tobii Pro Lab software. "Real-World Mapping" only showed acceptable accuracy when the static image's "quality" - not only its resolution – was high enough. For this reason, we used the original Garmin 1000 instrument panel image, instead of a screenshot of the recorded movie from the Tobii Pro Glasses 2 eye-tracker (Tobii Technology AB, Sweden). Furthermore, the use of the original instrument panel image was necessary to avoid other image artifacts such as blur, image distortion, or color misrepresentation. Raw data (Participant name, Recording name, Recording duration, Recording Timestamp, Automatically-mapped gaze data score, Mapped eye movement type, Automatically-mapped gaze data X, Automatically-mapped gaze data Y) was extracted from Tobii Pro Lab in ".tsv-format" (tab-separated values).

### 2.1 Resemblance between the actual and instructed scan patterns (Model 1)

The model was developed with the intent of understanding whether the scan patterns were executed in the correct sequence as instructed. First, the flight test was subdivided into the different flight stages, corresponding to the flight test sequence exported from the open-source Behavioral Observation Research Interactive Software (BORIS, boris.unito.it) [11]. The taught scan patterns are composed of a sequence of instruments to be observed by the participant, and a particular order of scanning. For this analysis, seven Areas of Interest (AOI's) were indicated on a 1216 × 764-pixel (px) display: Speed (87 × 38 px); Altitude (106 × 38 px); Heading (71 × 33 px); Attitude Direction indicator (ADI: 142 × 36 px); Bank (434 × 155); Vertical Speed (68 × 315 px); Power (188 × 177 px) (Figure 1, right upper panel). Visual scan patterns indicating specific sequences of instruments that are pre-defined according to a specific flight stage, as instructed, were analyzed. To assess these patterns, a Visual Pattern Search method was developed (Figure 1, lower panel).

In this method, first the current flight stage is determined (e.g., TURN) which relates to an appropriate instructed scan pattern (ADI, SPEED, ALTITUDE, HEADING, ADI – in red). Next, the student's flight test is observed, and his/her tracked gaze points are analyzed based on x-y coordinates relative to the screen dimensions ([111,202]; [454,320]; . . . ). The gaze points are matched to their appropriate AOI's (ADI, SPEED, . . . ) (see Figure 1). Thereafter, each AOI is coded into a positive integer (1,6,. . . ).

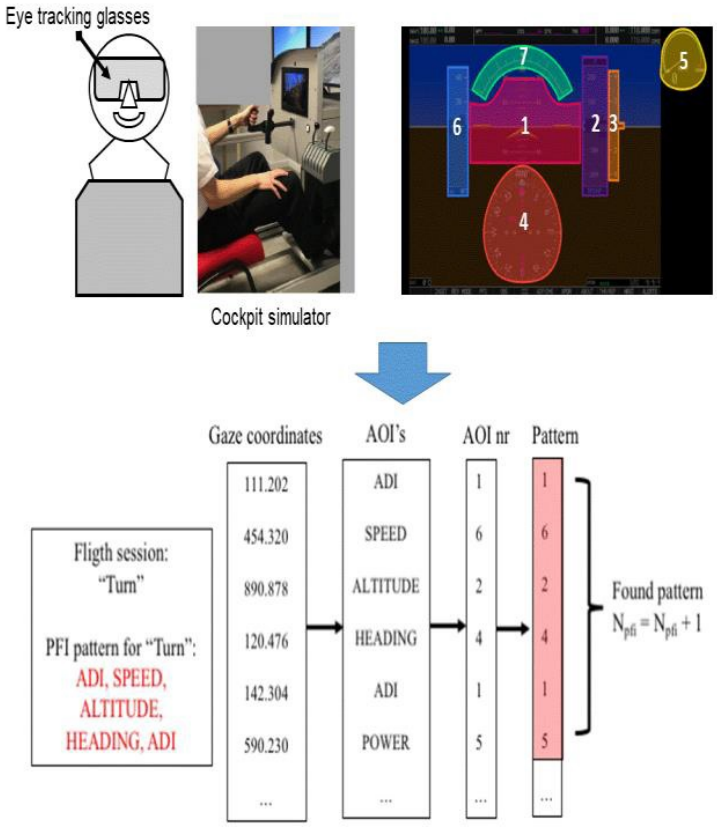


**Figure 1:** Model for matching between used and instructed scan patterns (Model 1). Area of interest (AOI) indication on the cockpit instrument panel are shown (right upper panel).

Finally, this sequence of integers – a large array, valid for the whole flight test – is looked at by utilizing a moving window approach for all reported instances of the current instructed scanning pattern. All matching patterns were counted ("Number of Patterns") and a score based on the ratio of the number of matching patterns over the total number of patterns used ("Order Score") was calculated:

$$O_s = \sum_{T=0}^{t_{flight}} \sum_{t=0}^{t_{stage}} \frac{N_{Scan}(F_S)}{N_{total}(F_S)}$$

where $t_{flight}$ is the total flight duration, $t_{stage}$ is the duration of the current stage (e.g. climb, decent, turn, etc.), $N_{Scan}(F_s)$ is the number of instances of the instructed scan pattern relevant to the current $F_S$, and $N_{total}(F_S)$ is the total number patterns that could fit in the current $F_S$. The order score values were normalized with a 100% match between the student's scan pattern and the taught scan pattern resulting in a score of 1 (i.e., the highest score possible).

## 2.2 Parafoveal information processing (Model 2)

*2.2.1 Gradient masks design.* For gradient mask design, new AOI's were defined, taking foveal as well as parafoveal vision into account. Gradient images centered around each instrument to define AOIs were used to create a meaningful representation of the human optical perception. Seven AOI's were defined on the same instruments as mentioned above, only this time the AOI's were overlapping circles (Airspeed; Altitude; Heading; ADI; Bank and Power – circles of 483 × 483 px) or ellipses (vertical

speed– an ellipse of 483 × 561 px). Each AOI was represented as an 8-bit grayscale image (255 tones) in which a shape – circle or ellipse – is centered at that instrument's centroid, with a radial gradient dimming from brightest in the middle (1 or RGB 255,255,255) to black (0 or RGB 0,0,0) as it approaches the edges. The gradient's size was specifically calculated so that it reflects the average size of a person's foveal and parafoveal vision. The essential assumption is that a person's visual acuity deteriorates in two linear curves, one with a certain inclination within the fovea and one with a higher inclination from the foveal edge to the parafoveal edge [12]. In this case, the fovea was considered as a cone-shaped depression in the central retina measuring 1.5 mm in diameter, corresponding to 5° of the field of vision [13]. The parafovea, in turn, was considered as a ring-shaped region surrounding the fovea with an outer diameter of 2.5 mm representing 8° of the field of vision [14]. The student pilots' field of view (FOV) corresponding to the foveal and parafoveal regions were calculated as such:

$$\begin{aligned} d &= 85 \text{ cm} \\ res &= 96 \text{ ppi} = 37.79 \text{ px/cm} \\ f_{fovea} &= 5^\circ = 0.0872665 \text{ rad} \\ f_{parafovea} &= 8^\circ = 0.139626 \text{ rad} \end{aligned}$$

with d as the distance from the viewer (Pilot) to the screen (Garmin G1000), res as the screen resolution, $f_{fovea}, f_{parafovea}$. If $L$ is considered as the pixel size of the mask applying the definition of radian, then:

$$L = d \cdot \alpha \cdot res$$

with $\alpha$ as the scope of these regions in a person's field of view. Finally, by taking $\alpha$ as $f_{fovea}$ and $f_{parafovea}$, respectively, we get:

$$\begin{aligned} L_{fovea} &= 85 \cdot 0.087 \cdot 37.79 = 280 \text{ px} \\ L_{parafovea} &= 85 \cdot 0.14 \cdot 37.79 = 450 \text{ px} \end{aligned}$$

These numbers were then used to produce the grayscale masks (see Figure 2).

*2.2.2 AOI matching.* Because the instrument panel was relatively small (< 22 degrees field of view (FOV)) and close to the pilot (< 85 centimeters), the AOI density was high. This factor was implemented in the analysis. As an example, let us consider the gaze points Ga, Gb, and Gc, directed at the instrument panel (see Figure 3). Following the standard algorithm, points Ga and Gb are checked and classified as being inside the SPEED and ADI instruments, respectively. The Gc point, in turn, would be classified in this case as being outside any AOI, which is, in a non-relevant area. In this study, we considered that in the small FOV space occupied by the instrument panel, it was likely that a certain gaze would always extract some form of information from an instrument, so an analysis of which instrument would be most likely to provide relevant information at a certain point was required. For this analysis, a continuous probability distribution, represented by the various gradients centered at each AOI was used:

$$P_{gaze} = a \cdot r + b$$

where $P_{gaze}$ is the gaze probability (the probability that the pilot is looking at a certain point), $r$ is the distance from the center point in the radial axis, and $a$ and $b$ are linear adjustment coefficients (see Figure 3). By using this algorithm, the Gc point was compared against the probability distribution and the mask with the highest value at that point would be considered to be the instrument targeted at that moment.

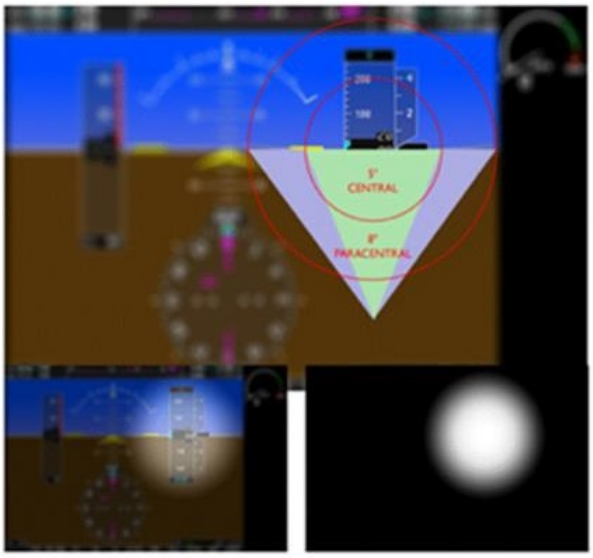


**Figure 2:** Greyscale masks after calculation of the parafoveal and foveal regions.


**Figure 3:** A schematic representation of three gaze points on the cockpit panel and the model representing the calculation for the field of view (FOV).

*2.2.3 Total gaze score.* For calculation of the total gaze score it was assumed that viewers (pilots) can extract essential information from several instruments located around their point of fixation within a certain (parafoveal) visual field. The total gaze score estimates the possibility that viewers (pilots) extracted information from essential instruments (e.g., instruments that need to be fixated as part of an instructed pattern) during execution of a specific flight maneuver. To determine the total gaze score, foveal as well as parafoveal vision was included. Using the above-mentioned masking technique, the flight test was subdivided into the different flight stages. A score was calculated based on the normalized value of the "gradient mask" (detailed description above) at the coordinates of that gaze point. Each gaze point had a specific score with which it was associated. This score was the summation of all the scores for the different instrument masks. Gaze points that were close to the instrument center, as indicated by the specific instructed pattern, received higher scores. The average of all those scores was the total score for that participant. Finally, the gaze point score was calculated:

$$G_S = \frac{1}{N} \sum_{T=0}^{t_{flight}} \sum_{t=0}^{t_{stage}} \sum_{i=0}^{N_{ins}} mask_i(x_{gaze}, y_{gaze})$$

With $t_{flight}$ as the whole flight simulation test, $t_{stage}$ as the current flight stage, $N_{ins}$ as the total instruments in the current flight test (according to the instructed pattern), $mask_i$ as the current "gradient mask" associated with an instrument, $x_{gaze}$ and $y_{gaze}$ as the current gaze coordinates, and

N as the total number of scores calculated for all different possible patterns suggested for that flight stage.

*2.2.4 Other gaze metrics.* Other eye-movement characteristics that were calculated were: number of dwells; average dwell time; and number of dwells per AOI. In line with Holmqvist et al. [15], a dwell was defined as one visit in an AOI, from entry to exit and returns to the AOI are counted as new dwells. Dwell time is then the duration gaze remained inside the AOI measured from entry to exit. The number of dwells was defined as the number of visits to an AOI. The average dwell time was calculated as the average of all the dwell times in a certain AOI during the task.

## 3 CASE STUDY

We tested our visual scoring tool on eye-tracking data recorded during a simulated flight task before (PRE) and after (POST) a short instruction session during which student pilots received information about specific visual scan patterns to use during different flight maneuvers. Participants were 18 student pilots who received instructions about specific visual scan patterns for different flight maneuvers at the CAE Aviation Academy Brussels. In total, eye-tracking measures were analyzed for 17 participants on the pre-test, whereas measures of the post-test were analyzed in 18 participants.

All participants were students at the academy and had already completed an entrance examination that consisted of a basic flying assessment (BFA, a simulated flying task during which participants receive verbal flying instructions). All participants provided written informed consent and the study was approved by the University's (KU Leuven) ethics committee (G-201504218).

Participants completed the BFA before and after receiving information about specific visual scan patterns for different flight maneuvers (pre- and post-test). The BFA consisted of a series of simulated flight tasks that were completed on a Garmin G1000 simulator. The task included 12 flight maneuvers that included: turns (2); roll outs (4); climbs (2); descents (2); and combinations of turns and climbs/descents (2). A recorded voice called out flight instructions for each maneuver (e.g., "descent with 1,000 feet per minute") and in between two different maneuvers the participants were instructed to fly straight and level at 3000 feet. The instructions were repeated when the computer noticed significant deviations from the instructed flight path (e.g., "please turn right with 20 degrees", when a participant is turning left instead). In total, the BFA lasted approximately 26 minutes with small variations across participants (±30 seconds) depending on how fast they completed the maneuvers or how many errors they made. During the BFA, participants were instructed to make specific scan pattern for each maneuver (e.g., climb, decent, roll out, turn, or a combination of different maneuvers) but were instructed to repeat a T-check scan pattern in a steady flight.

In addition to learning and applying theoretical scan patterns, participants were also instructed about the pitch-power table (for more information, see [16]) as well as learning the correct attitude a professional pilot should have (KSA: Knowledge, Skills, and Attitude). At the end of the BFA, participants received a final score in percentage. However, our findings revealed no significant PRE to POST improvement, neither in the order scores nor in the gaze-point scores; both $F \leq 2.11$; $p \geq 0.17$. Order scores were in general below 0.5 (Mean = 0.30 ± 95% CI [0.25, 0.36]). Total gaze scores were: 0.72 ± 0.12 (PRE) and 0.73 ± 0.12 (POST). Similarly, there were no significant PRE to POST changes in all other gaze metrics characteristics; all, $F \leq 1.03$; $p \geq 0.33$.

Further inspection revealed, nonetheless, a significant main effect for AOI, regarding both the number of dwells per AOI and average dwell duration within an AOI (both: $F \geq 12.88$, $p \leq 0.001$). With respect to the *number of dwells per AOI*, the ADI (2,823 ± 1,195) and altitude (2,784 ± 1,004) were the most visited AOIs and speed (182.3 ± 124.5) and vertical speed (328.5 ± 259.7) were the least visited AOIs. With respect to average dwell duration, dwells were on average longer on the speed

(339.3 ± 801.2 sec.) and vertical speed indicator (160.2 ± 164.8 sec.), whereas dwell times appeared to be the shortest on the ADI (12.9 ± 18.6 sec.) and altitude indicator (12.3 ± 17.1 sec); all $p < 0.001$.

## 4 DISCUSSION

In this article we describe an innovative visual scoring tool to unravel scan patterns used in the cockpit. With this tool two scan patterns: (1) based on the order of fixations in AOI's (cockpit instruments in this case) and (2) those implementing parafoveal information processing can be analyzed. The tool was developed to compare a standardized "perfect" scan pattern with recorded raw eye-tracking data. For this reason, the visual scoring tool's ideal use would be for training. Here we tested the algorithms, as a case study on pilot students that were instructed to use specific visual scan patterns during different flight maneuvers. Eye-tracking measures were collected before and after they received these instructions, during completion of the BFA, a simulated flying task. In this case study we aimed to examine whether student pilots adapt their visual scan patterns to those that were instructed and to what extent does this information influence gaze behavior.

### 4.1 Resemblance between the used and taught scan patterns (Model 1)

Our findings revealed that "order scores" were very low (around 0.30, whereas maximal adaptation to the scan pattern would result in a score of 1.0), suggesting that the participants did not use the instructed scan patterns. Due to this observation we might question the accuracy of our scoring tool. Although, literature has shown similar results after visual search training [17]. In this study, medical students were taught to analyze radiographs using a systematic scan pattern. The results indicated that in contrast to what was expected, medical students and residents who enrolled in the visual search training did not fully adhere to the systematic scan patterns they were taught, especially when an abnormality was clearly visible. Hence, it appears that both trainee radiologists and pilot students from CAE were unable to adapt their gaze according to the taught systematic scan patterns. This finding suggests that instructing students to perform expert-like gaze patterns may require more time and more repetitions before optimal scanning is to be achieved.

### 4.2 Parafoveal information processing (Model 2)

For calculation of the total gaze score we assume that the pilot extracted essential information from several instruments located around his/her point of fixation within a certain parafoveal visual field. In line with this assumption, a "total gaze score" was calculated to estimate the possibility that the observer extracts information from essential instruments (e.g., instruments that need to be fixated as part of an instructed pattern) during execution of a specific flight maneuver. Here (as opposed to "order scores"), relatively high scores were obtained (around 0.75, whereas optimal information extraction would be 1.0). Accordingly, it appears that using foveal vision may not be enough and that a model using both foveal and parafoveal vision may provide better assessment of pilots' gaze.

The observation that student pilots already use these patterns before receiving information about specific scan patterns to use during different flight maneuvers, might be explained partly by the pre-selection procedure conducted by the academy. All the student pilots in this study passed the entrance-exam of the Academy, which indicated that they knew how to conduct a flight in a simulator successfully. The participants' scanning behavior might be one of the reasons for successful completion of this exam.

In line with previous research, it might be possible that due to their experience with simulated flights, the student pilots were able to extract information from the instruments using their parafoveal vision [18–20]. They may have been able to divert their attention to the most important instruments,

without missing essential information from other instruments. However, this assumption should be considered with some caution. Specifically, it is likely that student pilots may not have yet achieved sufficient levels of expertise to effectively process information parafoveally. Published reports suggest that this skill develops with extended experience in the domain (e.g., radiology [18], sports [21], and chess [19]). In future, researchers should consider using complimentary methods to assess the extent to which information is processed via the parafovea in student pilots. A possible method to study parafoveal information processing is to work with blurred scenes. Fox et al. [22] applied this technique by blurring the parafoveal vision in a cockpit setting. The expert pilots performed worse when parafoveal vision was blurred, suggesting that they depended more so on this information (for a review of methods, see [23]). Furthermore, running the order score package on a blurred scene might also indicate interesting results. It can be expected that this score might increase in that case.

## 5 CONCLUSIONS

Findings from the case study suggested that using the visual scoring tool to analyze student pilots' raw eye-tracking could allow instructors to evaluate whether instructed scan patterns are strictly followed by student pilots after receiving instructions about these visual scan patterns. Taking parafoveal information processing into account (Model 2) appeared to improve the model based on foveal vision only (Model 1). Still, this model needs to be further validated in the future.

## ACKNOWLEDGMENTS

The authors would like to thank Tony De Wolf and Ken Evens from the CAE Oxford Aviation Academy, Brussels, Belgium for their help with the experimental part of this study.

## REFERENCES

[1] Angela T Schriver, Daniel G Morrow, Christopher D Wickens, and Donald A Talleur. Expertise differences in attentional strategies related to pilot decision making. *Human Factors*, 50(6):864–878, 2008.

[2] Christopher D Wickens. Situation awareness and workload in aviation. *Current directions in psychological science*, 11(4):128–133, 2002.

[3] Gal Ziv. Gaze behavior and visual attention: A review of eye tracking studies in aviation. *The International Journal of Aviation Psychology*, 26(3-4):75–104, 2016.

[4] Stephanie Brams, Ignace TC Hooge, Gal Ziv, Siska Dauwe, Ken Evens, Tony De Wolf, Oron Levin, Johan Wagemans, and Werner F Helsen. Does effective gaze behavior lead to enhanced performance in a complex error-detection cockpit task? *PloS one*, 13(11), 2018.

[5] Melanie Diez, Deborah A Boehm-Davis, Robert W Holt, Mary E Pinney, Jeffrey T Hansberger, and Wolfgang Schoppek. Tracking pilot interactions with flight management systems through eye movements. In *Proceedings of the 11th International Symposium on Aviation Psychology*, volume 6. Citeseer, 2001.

[6] Carolina Diaz-Piedra, Hector Rieiro, Alberto Cherino, Luis J Fuentes, Andres Catena, and Leandro L Di Stasi. The effects of flight complexity on gaze entropy: An experimental study with fighter pilots. *Applied ergonomics*, 77:92–99, 2019.

[7] Jonathan Allsop and Rob Gray. Flying under pressure: Effects of anxiety on attention and gaze behavior in aviation. *Journal of Applied Research in Memory and Cognition*, 3(2):63–71, 2014.

[8] Vsevolod Peysakhovich, Olivier Lefrançois, Frédéric Dehais, and Mickaël Causse. The neuroergonomics of aircraft cockpits: the four stages of eye-tracking integration to enhance flight safety. *Safety*, 4(1):8, 2018.

[9] S Scanella, Vsevolod Peysakhovich, Florian Ehrig, and Frédéric Dehais. Can flight phase be inferred using eye movements? evidence from real flight conditions. In *18th European Conference on Eye Movements*, 2015.

[10] Eric Fielding, Andrew W. Lo, and Jian Helen Yang. The national transportation safety board: A model for systemic risk management. 2010. Available at SSRN: https://ssrn.com/abstract=1695781.

[11] Olivier Friard and Marco Gamba. Boris: a free, versatile open-source event-logging software for video/audio coding and live observations. *Methods in Ecology and Evolution*, 7(11):1325–1330, 2016.

[12] M D Crossland. Acuity. In *The retina and its disorders*, pages 1–6. Besharse, Joseph and Bok, Dean, 2011.

[13] Michel Millodot. *Dictionary of Optometry and Vision Science E-Book*. Elsevier Health Sciences, 2017.

[14] William H Swanson and Gary E Fish. Color matches in diseased eyes with good acuity: detection of deficits in cone optical density and in chromatic discrimination. *Journal of the Optical Society of America A*, 12(10):2230–2236, 1995.

[15] Kenneth Holmqvist, Marcus Nyström, Richard Andersson, Richard Dewhurst, Halszka Jarodzka, and Joost Van de Weijer. *Eye tracking: A comprehensive guide to methods and measures*. OUP Oxford, 2011.

[16] Adam Marshall Thoreen. Primary flight display pitch-and power-based unreliable airspeed symbology, March 4 2014. US Patent 8,665,120.

[17] Ellen M Kok, Halszka Jarodzka, Anique BH de Bruin, Hussain AN BinAmir, Simon GF Robben, and Jeroen JG van Merriënboer. Systematic viewing in radiology: seeing more, missing less? *Advances in Health Sciences Education*, 21(1):189–205, 2016.

[18] David Manning, Susan Ethell, Tim Donovan, and Trevor Crawford. How do radiologists do it? the influence of experience and training on searching for chest nodules. *Radiography*, 12(2):134–142, 2006.

[19] Eyal M Reingold, Neil Charness, Marc Pomplun, and Dave M Stampe. Visual span in expert chess players: Evidence from eye movements. *Psychological Science*, 12(1):48–55, 2001.

[20] Ludo W van Meeuwen, Halszka Jarodzka, Saskia Brand-Gruwel, Paul A Kirschner, Jeano JPR de Bock, and Jeroen JG van Merriënboer. Identification of effective visual problem solving strategies in a complex visual domain. *Learning and Instruction*, 32:10–21, 2014.

[21] Werner F Helsen and Janet L Starkes. A multidimensional approach to skilled perception and performance in sport. *Applied Cognitive Psychology: The Official Journal of the Society for Applied Research in Memory and Cognition*, 13(1):1–27, 1999.

[22] Julianne Fox, David Merwin, Roger Marsh, George McConkie, and Arthur Kramer. Information extraction during instrument flight: An evaluation of the validity of the eye-mind hypothesis. In *Proceedings of the Human Factors and Ergonomics Society Annual Meeting*, volume 40, pages 77–81. SAGE Publications Sage CA: Los Angeles, CA, 1996.

[23] A Mark Williams and K Anders Ericsson. Perceptual-cognitive expertise in sport: Some considerations when applying the expert performance approach. *Human movement science*, 24(3):283–307, 2005.